AMERICAN UNIVERSITY OF BEIRUT

ASSESSING THE IMPACT OF DIFFERENT SIZED PARTICLES ON THE EFFICIENCY OF PHOTOVOLTAIC CELLS

by
DINA FARIZ SALEEM

A thesis
Submitted in partial fulfilment of the requirements
for the degree of Master of Science in Energy Studies
to the Department of Mechanical Engineering
of the Maroun Semaan Faculty of Engineering and Architecture
at the American University of Beirut

Beirut, Lebanon
December 2020

AMERICAN UNIVERSITY OF BEIRUT

ASSESSING THE IMPACT OF DIFFERENT SIZED PARTICLES ON THE EFFICIENCY OF PHOTOVOLTAIC CELLS

by
DINA FARIZ SALEEM

Approved by:

Dr. Ibrahim Alameddine, Assistant Professor
Department of Civil and Environmental Engineering ______________________
Advisor

Dr. Nesreene Ghaddar, Professor
Department of Mechanical Engineering ______________________
Member of Committee

Dr. Kamel Aboughali, Professor]
Department of Mechanical Engineering ______________________
Member of Committee

Date of thesis defense: [December 21, 2020]

AMERICAN UNIVERSITY OF BEIRUT

THESIS RELEASE FORM

Student Name: Saleem_ _ _ _ _ _ Dina_ _ _ _ _ _ _ Fariz_ _ _ _

Last First Middle

I authorize the American University of Beirut, to: (a) reproduce hard or electronic copies of my thesis; (b) include such copies in the archives and digital repositories of the University; and (c) make freely available such copies to third parties for research or educational purposes:

☐ As of the date of submission

☒ One year from the date of submission of my thesis.

☐ Two years from the date of submission of my thesis.

☐ Three years from the date of submission of my thesis.

Dina Saleem_______________________ January 11, 2021

Signature Date

ABSTRACT
OF THE THESIS OF

Dina Fariz Saleem for Master of Science in Energy Studies
Major: Mechanical Engineering

Title: Assessing the Impact of Different Sized Particles on the Efficiency of Photovoltaic Cells

The global capacity of solar panels installed during the last decade was estimated at 462 GW, with the total global capacity reaching 485 GW in 2018 (International Renewable Energy Agency (IRENA), 2019). Moreover, the rate at which renewable energy is being utilized has been witnessing a continuous growth over the past seven years, with an average annual growth rate of 8.3% (International Renewable Energy Agency (IRENA), 2019). As the sector continues to grow, there is a need to better quantify the effects of environmental factors (such as heat, wind, humidity and dust) on the efficiency of solar panels. This is of particular importance for the Middle East and North Africa (MENA) region that has a high potential to integrate solar energy within its existing energy sources. Yet, the region experiences frequent dust storms and high levels of urban pollution that can impact energy production. Previous work has shown that dust size and the rate of its deposition are two important factors affecting PV efficiency. Several experimental studies have attempted to quantify the impact of dust particle size on PV efficiency; yet few have worked with dust sizes below 10 µm. In this paper, we set up an experimental design that allowed us to assess and quantify the impact of dust, with particle sizes ranging between 0.1 and 8 µm, on the efficiency of PV cells. Our results showed that efficiency dropped as the concentration of particles in the air increased; yet the rate of the drop was a function of particle size. The largest reduction in efficiency occurred for particles whose diameter was between 2 µm and 10 µm. A linear regression model was developed to explain the relationship between efficiency reduction and the concentration of particles given their particles size. The model was able to explain around 71% of the observed variability in the sampled data.

TABLE OF CONTENTS

ABSTRACT 1

ILLUSTRATIONS 3

TABLES 4

Chapter

I. INTRODUCTION 6

II. METHODOLOGY 20

A. Experimental setup 20

1. Sun Simulator 21

2. PV System 22

3. Particle Generator or CMAG 23

4. Optical Particle Sizer Spectrometer or OPS 24

5. Determining the duration of the experiment 25

6. Efficiency 26

B. Statistical analysis 28

III. RESULTS AND DISCUSSION 30

IV. CONCLUSION AND LIMITATIONS 37

REFERENCES 39

ILLUSTRATIONS

Figure Page

1: Dust deposition rate on the PV panels mounted on the windward building roof – Adapted from (Lu et al., 2016) 16

2. : An illustration of the lab experiment setup (Adapted from (Jiang et al., 2011)) 20

3: An illustration of how the irradiation was measured inside the chamber by the pyranometer (left) and the corresponding reading of the meter (right) 21

4: The Class II Pyranometer (PMA2144, PMA2100, Solar Light Company Inc.) used 22

5: An illustration of the Optical Particle Sizer (OPS) Reading for Test 28 25

6: Sample I-V curve for the used silicon cell 27

7: (a) Efficiency reduction as a function of concentration ($\mu g/m^3$) and particle size; (b) Deposition density (g/m2) as a function of concentration ($\mu g/m^3$) and particle size 32

8: Log of efficiency reduction as a function of log of deposition density 33

9: Deposition density for different size particles 36

TABLES

Table Page

1: Solar power potential in the MENA region [adapted from (Global Solar Atlas; IEA Atlas of Energy; International Renewable Energy Agency (IRENA))] 7

2: Summary of previous studies that have reported on the effect of dust on PV cell performance 11

3: Particle generator parameters associated with several size particles.......................... 23

4: Efficiency reduction and deposition density under the three particle size categories generated... 32

5: Coefficients of the linear regression model 34

ABBREVIATIONS

MENA	Middle East and North Africa
PM	Particulate Matter
PV	Photovoltaic cells
NR	Not Reported
NA	Not Applicable

CHAPTER I

INTRODUCTION

Photo voltaic (PV) cells technology is continuously advancing. PV cells generate power by converting the incoming energy of photons into electricity rather than heat (Mekhilef, Saidur, & Kamalisarvestani, 2012). This occurs because the electrons receiving the energy from the photons get liberated and move across the crystal (Mekhilef et al., 2012). Since the PV cell is connected to a circuit, electrons move as an electric current and produce work. Over the past decade, the installed global capacity of solar panels was estimated to have reached 462 GW, with the total installed capacity exceeding 485 GW in 2018 (International Renewable Energy Agency (IRENA), 2019). In 2017 alone, the annual growth rate in installed capacity exceeded 30% (International Renewable Energy Agency (IRENA), 2018), much higher than the growth experienced in the entire renewable energy sector that grew by around 8% per year over the past seven years (International Renewable Energy Agency (IRENA), 2019). China continues to lead the way in terms of the global solar capacity, whereby its new installations in 2017 accounted for more than half of all the new global capacity installed during that year (53 GW). In the Middle East region, Turkey has been leading with regards to solar energy production, with new installations of 2.6 GW in 2017 alone (International Renewable Energy Agency (IRENA), 2018). As shown in Table 1, the MENA region has a high potential with regards to its solar energy; yet most countries still fail to capitalize on that resource. Many countries in the region have very low energy self-sufficiency and very low operating solar output. This suggests that the high potential of solar power production in the MENA is being improperly utilized towards improving the overall power production in the region.

Table 1: Solar power potential in the MENA region [adapted from (Global Solar Atlas; IEA Atlas of Energy; International Renewable Energy Agency (IRENA))]

Country	Overall energy self-sufficiency (2017)	Installed Solar PV capacity (2019) in MW	Solar Electricity Generation (2018 and 2019) in GWh	Direct Normal Irradiation (kWh/m^2)
Turkey	25	5,995	7,800	1022 – 2337
Jordan	4	1,240	1,476	2045 – 2191
Lebanon	2	56.37	83.6	1607 – 2629
Egypt	84	1,647	69.1	1899 – 2775
Cyprus	6	128.6	199.5	1753 – 2264
Kingdom of Saudi Arabia	306	344.4	65	1461 – 2922
United Arab Emirates	339	1,785	1,076	1680 – 2118
Morocco	9	204.1	30.8	1680 – 2556
Algeria	275	423	373.6	1680 – 2556
Bahrain	160	6.349	8.25	1570 – 1862
Iran	162	367.1	221.8	1095 - 2410
Iraq	388	215.5	376.5	1680 - 2410
Kuwait	477	43.34	70.69	1680 - 1972
Libya	404	5.11	7.791	1972 - 2556
Malta	3	153.8	189.6	1716 - 1862
Oman	295	8.291	15.71	1753 - 2483
Qatar	522	5.1	8.364	1607 - 1899
Syria	46	2.467	2.424	1753 - 2629
Tunisia	49	62.08	58	1534 - 2264
Yemen	54	250	732	1387 – 2702

Several factors are known to affect the efficiency of solar cells. The performance of photovoltaic cells can be impacted by several environmental factors, including temperature, wind speed, humidity, solar irradiance and dust (Micheli, Muller, & Kurtz, 2016). The photovoltaic conversion process is highly dependent on the module’s temperature, which in turn depends on several meteorological factors such as ambient temperature, wind speed, solar irradiance, humidity, and dust (J. K. Kaldellis, Kapsali, & Kavadias, 2014). At a fixed solar radiation of 1,000 W/m^2, lower ambient temperatures improve the solar PV efficiency (Fesharaki, Dehghani, Fesharaki, & Tavasoli, 2011). At an irradiation of 1000 W/m^2, Rahman, Hasanuzzaman, and Rahim (2015) reported that the electrical efficiency was reduced by 0.06% for every 1 °C rise in the PV cell temperature. Jiang, Lu, and Sun (2011) showed that increasing the incoming solar irradiation generated from a sun simulator caused a degradation in the PV efficiency due to overheating of the module. Meanwhile, Abderrezek and Fathi (2017) reported that the PV efficiency was affected by variations in the light transmission level and the glazing temperature. J. K. Kaldellis et al. (2014) showed that changes in wind speed affected efficiency, whereby an increase in wind speed reduced the difference between the PV cell temperature and the ambient temperature. Mekhilef et al. (2012) reported that increases in wind speed and humidity resulted in promoting dust deposition and thus caused an exponential drop in the PV performance. They found that humidity, wind speed, and dust deposition interacted together and thus their effect on PV efficiency was non-linear.

Among the aforementioned environmental factors, dust is also known to play an important role with regards to the performance of solar panels. For particles to be considered as dust, their diameter size should be 500 µm or less (Mani & Pillai, 2010). The source of the dust in the atmosphere can be either of natural or anthropogenic. The former includes volcanic eruptions and weather related phenomena such as wind induced dust storms, while the latter includes traffic related emissions, combustion processes, and pedestrian activities *(Mekhilef et al., 2012)*. Reported reductions in PV performance vary significantly between studies; they range from less than 1 % to an excess of 65 % (Mekhilef et al., 2012). Several studies (Table 2) have linked the drop in PV efficiency to dust characteristics such as size, chemical properties, shape, weight, etc. In terms of dust size, course particles have been shown to play a significant role in inhibiting the transmittance of light, thus, reducing the efficiency of solar cells. A study by Abderrezek and Fathi (2017) attempted to quantify the effect of different dust types on the efficiency of PV cells. They used a variety of dust sources, including sand (230.5 µm), red soil (particle size ≤150 µm), limestone (particle size ≤60 µm), salt (3191 µm), and ash (particle size ≤10 µm). Their results showed that variations in the physical parameters of the dust, such as its grain size and type, affected light transmission and the temperature of the PV and accordingly influenced the modules' performance. J. Kaldellis and Kapsali (2011) studied the effect of ash (≤10 µm), limestone (≤60 µm), red soil (≤150 µm) on the efficiency of a poly-crystalline silicon cell. They found that the red soil caused the highest reduction in PV efficiency (2.3%), followed by limestone (1.2%), and lastly carbon ash at 0.7%. However, El-Shobokshy and Hussein (1993b) reported that fine particles reduced the performance of PV cells more than coarser particles when they studied the effect of limestone Grade I (80 µm), limestone grade II (60 µm), limestone grade III (50 µm), cement (10 µm), and carbon (5 µm) in an indoor lab-based experiment. Gutiérrez et al. (2018) have underscored the importance of including aerosols in future PV performance scenarios for the Euro-Mediterranean area because of the non-negligible impact they have on PV performance. In fact, their analysis showed that the impact of aerosols on the annual PV production loss can range from 0 to 16% in the Netherlands and reach up to 20% in some regions of Africa and Syria-Iraq. During the simulation of the brightening period over Europe, they reported that reducing anthropogenic aerosols could potentially increase energy production by

2000 (kW h)/(kW p) in a PV lifetime, where kW h is defined as kilowatt hour equivalent to 3600 kilojoules and represents the total amount of electricity the system actually generates in a year; while kW p is kilowatt peak of a system and it represents the rate at which the solar electricity system generates energy at peak performance, for instance, at noon on a sunny day.

Table 2: Summary of previous studies that have reported on the effect of dust on PV cell performance

Study	Year	Dust size (diameter in µm)	Location	Type of cells	Results/efficiency reduction
(Abderrezek & Fathi)	2017	• Sand: 230.5 µm • Soil: 128.466 µm • Salt (NaCl): 3191 µm • Cement: 10 µm • Gypsum: 18.332 µm • Ash: 9.696 µm	Two experimental studies: Indoors lab-based and Outdoors	• 150 W solar panel - monocrystalline SUNTECH STP020S-12/Cb	• The solar spectrum decreased linearly with the increase of dust concentration, thus light is more diffused under glazing • Dust particles with small grain size had a stronger influence on solar spectrum and the light transmission as compared with big size dust particles • Small dust particles placed on the module surface tend to occupy more places compared with larger dust particles with same weight • Finer particles from a given dust have a more deteriorating effect than that of the coarser one due to the uniform manner in which finer particles are distributed • Ash and soil were found to overheat the module more than others. Salt decreased the module temperature
(J. Kaldellis & Kapsali)	2011	• Ash:≤10 µm • Limestone: ≤60 µm • Red soil: ≤150 µm	Indoor lab-based	• Poly-crystalline silicon	• Red soil (≤ 150 µm) caused the PV efficiency degradation to increase the most at 2.3%, followed by limestone (≤ 60 µm) at 1.2% then carbon ash (≤ 10 µm) at 0.7%
(El-Shobokshy & Hussein)	1993	• Limestone Grade I: 80 µm • Limestone Grade II: 60 µm • Limestone Grade Ill: 50 µm • Cement: 10 µm • Carbon: 5 µm	Indoor lab-based	• NR	• When comparing dusts of the same constituents but with different sized particles, dust with fine particles reduced the performance of PV cells more than that those with coarser particles
(El-Shobokshy & Hussein)	1993	• d_p= 80 µm and σ_g = 1.6 where d_p being the number of median diameter and σ_g the geometric standard deviation	Indoor lab-based	• A panel of commercial silicon cells	• As the accumulation of dust particles (of size 80 µm) reached about 250 g/m^2, the short circuit current decreased by 82%. • The increase in the temperature of the photovoltaic cell caused a noticeable reduction in the fill factor, whether the PV cell was cleaned or not.

Study	Year	Dust size (diameter in µm)	Location	Type of cells	Results/efficiency reduction
(Gutiérrez et al.)	2018	A detailed interannual aerosol dataset is used in the climate simulations, and includes five different aerosol species: • Sea Salt • Black carbon • Sulfate • Organic Carbon • Desert Dust	Outdoor	• NR	• The annual PV production loss is dependent on the area and typology of the tracking system. The effect of aerosols on the mentioned loss ranges from 0% to 16% in the Netherlands, while it reaches 20% over regions of Africa and Syria-Iraq. • The effect of aerosols is of high importance when studying PV production at large time scales over the Euro-Mediterranean area. • PV potential could be seriously affected in highly polluted areas. The non-negligible impact of aerosols on PV production suggests that the inclusion of aerosols in future scenarios is a necessity for solar energy assessment.
(Micheli et al.)	2016	• Aerosols that are less than 100 µm in diameter (TSP) • Airborne particulate matter less than 2.5 µm in diameter (PM2.5) • PM10	Outdoors	• Monocrystalline silicon PV cells	• Soiling ratio is defined as the ratio of daily average short circuit current of a soiled PV cell to that of a clean PV cell • PM_{10} had the best correlation with the average daily SRatio (soiling ratio) for the tested sites (R^2 = 0.95) • A good correlation also existed between $PM_{2.5}$ and the average daily SRatio (R^2= 0.70).
(Bergin, Ghoroi, Dixit, Schauer, & Shindell)	2017	• The mass size distribution reveals that 90% of the particles had diameters less than 30 µm • 50% of the particles had diameters less than 14.65 µm • Around 10% of the particles had diameters less than 2.84 µm	Outdoors	• 10 kWp Solar PV (Thin-film, CIS) System – L Block • 10 kWp Solar PV (Multicrystalline Silicon) System	• For solar panel where surface cleaning occurred every 20 - 30 days, power generation increased on average by ~ 50% after each cleaning • Much of the atmospheric PM burden in northern India was influenced not only by wind-blown and fugitive dust but also by anthropogenic sources, including solid biofuel and trash/refuse burning, mobile source emissions, and power generation from fossil fuel combustion that emits PM compounds, including organic (OC) and elemental carbon (EC/BC), as well as ionic species • The influence, per unit mass, of natural dust on solar PV transmittance is weaker than that of combustion-related particulate matter due to its larger particle size and smaller upscatter fraction. Although the deposited anthropogenic PM accounted for only ~8% of the total mass of dust deposited, it was estimated to be

Study	Year	Dust size (diameter in μm)	Location	Type of cells	Results/efficiency reduction
					responsible for nearly 50% of the change in transmittance
(Jiang et al.)	2011	• The test dust had a multidistribution of sizes from 1 μm to 100 μm. The sum volume of dust less than 20 mm was 74% and the dust with the highest volume had a size 20 mm (at 20%)	Indoor lab-based	• Mono-crystalline silicon covered with white glass • Poly-crystalline silicon covered with Epoxy • 3- Amorphous silicon covered with white glass	• As dust deposition density increased from 0 to 22 g/m^2, the short circuit current (Isc) was reduced from 100% to 78% of its maximum value, while the reduction of output efficiency grew from 0 to 26%. • The difference between different PV cell types was low
(Lu, Lu, & Wang)	2016	• PM10 • PM2.5 • 50 μm dust	Outdoor	• NR	• The rate of dust deposition first increased then decreased with the increase of dust particle size. • For 10 μm dust, the maximum deposition rate was reported to be 0.28% and for 50 μm dust, the minimum deposition rate was around 0.13%. • Gravity had a significant impact on the rate of dust deposition for large particles (dp > 5 μm), while it had very little effect on small particles with dp less than 5 μm
(Wang, Meng, & Chen)	2020	• PM2.5 • 53 – 75 μm dust	Outdoor	• Two pieces of PV panels, south-facing, with a tilt angle of 22°c. Total surface area of the PV modules is 5.625 m^2	• Pollutant particles suspended in the atmosphere increase the dust deposition rate on solar panels • The amount of solar radiation is exponentially correlated to the PM2.5 concentration by the following relationship: y=0.5495e−0.004x. • As PM2.5 concentration increases from 196 μg/m^3 to 266 μg/m^3, solar radiation decreases 0.237 kW to 0.193 kW • Deposition of atmospheric dust lead to greater efficiency reduction compared to that of an equivalent amount of artificial dust. • The size of atmospheric dust particles is smaller than that of artificial dust, which consists of clay-generated particles with a size range of 53 – 75 μm.
(Zhou et al.)	2019	• $PM_{2.5}$ (particles with diameter less than 2.5 μm) and PMC (particles whose diameter is between 2.5 μm and 10 μm)	Outdoors	• NR	• Fine particles had a greater up scatter fraction and as a result had a greater influence on panel transmittance as compared to coarse particles • A strong correlation was found between the change in solar panel transmission and the dust deposition amount

Study	Year	Dust size (diameter in µm)	Location	Type of cells	Results/efficiency reduction
(Boyle, Flinchpaugh, & Hannigan)	2016	• PM10 • PM2.5	Outdoor	• Glass plates similar to those used as PV panel cover plates	• PM10 concentration contributed in 9% of the variability of mass accumulation, while PM2.5 did not play a significant role in predicting mass accumulation and therefore efficiency reduction
(Roumpakias & Stamatelos)	2020	• PM10	Outdoor	• 99.84 kWp grid-connected	• The impact of ambient aerosol concentration levels on the efficiency of PV cells is more complex than studying the soiling effect, and the former requires more study • High normalized efficiency corresponds to high values of clearness index as well as moderate values of clearness index, which in turn correspond to PM10 concentrations < 50 µg/m^3
(Zhang, Li, Yu, & Xu)	2016	• PM2.5	Outdoor	• NR	• PV power outputs decreased by 6.5%, 7% and 30.3% under the defined PM2.5 good, slightly polluted, severely polluted conditions, respectively. One-unit increased percentage in the PM2.5 concentration decreased the solar irradiation by about 4%, 7% and 9% for the good, slightly polluted and severely polluted groups, respectively.
(Saidan, Albaali, Alasis, & Kaldellis)	2016	• Between 0.4 and > 1.2 µm	Indoor lab-based and Outdoors	• 3 identical panels used • Each panel consisted of 33 mono-crystalline silicon cells connected in series	• Solar panels exposed to dust during a time range from one day to one month had their maximum current decrease by 6.9% to 16.4% respectively
(Ramli et al.)	2016	• NR	Outdoors	• Two PV modules in parallel, a single PV 100Wp and 5 × 20 Wp	• After two weeks of exposure, the power of PV panels was reduced by 10.8% compared to cleaned panelsDuring the dry season, a very thin layer of dust reduced solar power conversion by 40%
(Neher et al.)	2017	• Aerosol size was not included as a variable, but attributed as an important factor	Outdoor	• Polycrystalline silicon PV module	• Daily reduction on PV yields range from 2% to 48% with a mean of 14%, and the maximum of 48% corresponding to an expected sandstorm event • Decreasing daily PV yields as a result of increasing atmospheric aerosol load is of substantial concern in the light of anthropogenic effects on atmospheric aerosol concentration

Dust deposition has been suggested to play a significant role in reducing the efficiency of PV cells. A study conducted by Jiang et al. (2011) showed that when the dust deposition density for dusts with sizes ranging between 1 µm and 100 µm increased from 0 to 22 g/m^2, the solar PV short circuit current was reduced from 100% to 78% of its maximum value, while the reduction in output efficiency increased from 0 to 26%. El-Shobokshy and Hussein (1993a) reported that the short circuit current decreased by 82% as the accumulation of dust particles of size 80 µm reached about 250 g/m^2. Moreover, they reported that the increase in the temperature of the photovoltaic module itself caused a remarkable reduction in the fill factor (defined as the ratio of maximum obtainable power to the product of the open-circuit voltage and short-circuit current), whether the PV cell was cleaned or not. Meanwhile, Lu et al. (2016) studied the effect of several dust sizes and quantities on the dust deposition rates by investigating deposition over a wider range of dust sizes. They showed that the rate of dust deposition initially increased as dust particle size increased up until 10 µm, and then decreased as dust particle size increased from 10 µm till 50 µm as shown in Figure 1. They found that gravity played a significant role in the rate in dust deposition for large particles ($dp > 5$ µm), while its role on small particles was marginal. Their study developed a simple empirical model (Equation 1) that described the decline of solar panel efficiency as a function of longer exposure to dust time. Their model, similar to the one developed by (Jiang et al., 2011), indicated that the rate of the decline increased as the size of the dust particles increases.

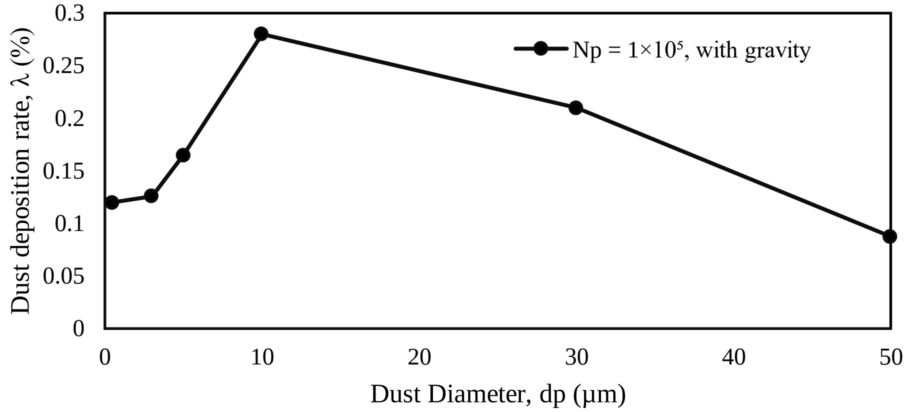

Figure 1: Dust deposition rate on the PV panels mounted on the windward building roof – Adapted from (Lu et al., 2016)

$$\frac{E_{reduction}}{E_{clean}} = \kappa\rho_{deposition} = \kappa\,\frac{N_d}{t_d}\,\frac{m_p}{S_d}\,T \times 100\% = \kappa\frac{\lambda N_p \pi \rho_p d_p^3}{6 t_d S_d}\,T \times 100\% \qquad \text{Equation 1}$$

where $E_{reduction}$ and E_{clean} are the PV output efficiencies with or without dust pollution, $\rho_{deposition}$ (g/m^2) is the dust deposition density, κ is the fitting factor from the experimental data, $\frac{N_d}{t_d}$ is the number of particles deposited in the time period t_d, m_p is the mass of each dust particle, S_d is the area of the PV panels. S_d is the area of the windward building roof by which the mass of the dust deposited on the PV panels is calculated, ρ_p is the dust density, T (day) is the exposure time. Under this model, the PV efficiency ratio decreases with the increase of dust particle size. The study concluded that the larger particles tended to have a higher dust deposition density, which in turn affected the drop in efficiency.

Neher et al. (2017) also studied the influence of aerosols on PV production, using an atmospheric radiative transfer and a PV power model. They ran their model on a Sub-Saharan region – the City of Niamey in Niger. Their results illustrated that the daily reduction on PV yields ranged between 2% and 48%, with a mean of 14%. They predicted a maximum reduction of 48% during a sandstorm event.. Boyle et al. (2016) conducted field measurements at two sites in Colorado for more than one year and measured the airborne $PM_{2.5}$ and PM_{10} mass accumulation and built a soiling prediction model (Equation 2). Their study found that PM_{10} concentrations were poor predictors alone of mass accumulation. When adding temperature and wind speed to the list of variables, the prediction of mass accumulation was improved and 26% of the variability could be accounted for. However, $PM_{2.5}$ and relative humidity were not significant predictors of mass accumulation.

$$\Delta\tau = 34.37 \mathrm{erf}\,(0.17\omega^{0.8473}) \qquad \text{Equation 2}$$

Where $\Delta\tau$ is defined as the transmission loss caused by deposited particles in percent, erf is the Gauss error function, and ω is the total dust deposition density in g/m^2. Meanwhile, Wang et al. (2020) concluded that pollutant particles suspended in the atmosphere increased the dust deposition rate on solar panels. They also investigated the influence of air quality on solar radiation and solar panels performance. In their study, PV cells were placed on a building roof in Shanghai, a city that suffers from severe particulate pollution. They found that dust resulted in a substantial loss in the solar panels' power generation with a maximum loss of 35.23% in the power generation efficiency.

Furthermore, they found that that the solar radiation exponentially decayed with the $PM_{2.5}$ concentration (Equation 3):

$$y=0.5495e^{-0.004x} \qquad \text{Equation 3}$$

Where y is the average hourly solar radiation and x is the $PM_{2.5}$ concentration.

Roumpakias and Stamatelos (2020) found that the impact of ambient aerosol concentrations on the efficiency of PV cells was more complex than just accounting for the soiling effect. Their study highlighted the need to account for the variability in the spectral distribution based on many factors present in the content of the atmosphere, such as, different gases, humidity, particles, among others. Moreover, atmospheric pressure was found to influence the spectrum of light reaching the ground and therefore impacted PM performance. Zhang et al. (2016) reported that the PV power output decreased by 6.5%, 7% and 30.3% when the $PM_{2.5}$ levels were considered to be good (between 35 and 75 μg/m^3), slightly polluted (between 75 and 115 μg/m^3), and severely polluted conditions (> 115 μg/m^3), respectively. Micheli et al. (2016) found that the correlation between the soling ratio and PM_{10} was stronger as compared to that associated with $PM_{2.5}$ (R^2 being 0.95 and 0.70 respectively). Zhou et al. (2019) performed outdoors experiments to study the effect of soiling on solar panels transmittance at different locations and under different conditions. Their results concluded that the performance of the panels was more affected by $PM_{2.5}$ (particles size ≤ 2.5 μm) as compared to PMC (2.5 μm < particles size ≤ 10 μm). Saidan et al. (2016) conducted indoor lab-based and outdoors experiments to assess the impact of particles sized between 0.4 and 1.2 μm. They concluded that solar panels exposed to dust during a time range from one day to one month had their maximum current decrease by 6.9% to 16.4% respectively.

This study aims to assess experimentally the effect of different sizes (0.1 – 10 μm) of fine dust particles on the efficiency of photovoltaic cells in a controlled environment. It also assesses the impact of increasing dust concentrations in the air on reducing output efficiency. Our work aims to fill a gap in the literature via experimental testing, where previous experimental studies have mostly worked on assessing the impacts of dust with diameters greater than 20 μm on PV efficiency and focused their work on quantifying the effect of varying deposition densities rather than the actual PM concentrations and sizes. The work provides more insight on how urban air pollution, with high concentrations of fine to ultrafine particulate matter, may affect PV efficiencies in global cities suffering from poor air quality.

CHAPTER II

METHODOLOGY

A. Experimental setup

The experimental setup was developed based on the system proposed by Jiang et al. (2011) (refer to Figure 2). It included four main components: 1) a sun simulator, 2) a PV system, 3) a particle generator, 4) and an optical particle sizer spectrometer. The setup was fitted in a test chamber 0.3 m (length) by 0.3m (width) by 0.5m (height). The chamber was made from Plexiglas, which is highly transparent and anti-static to simulate a natural dust deposition process.

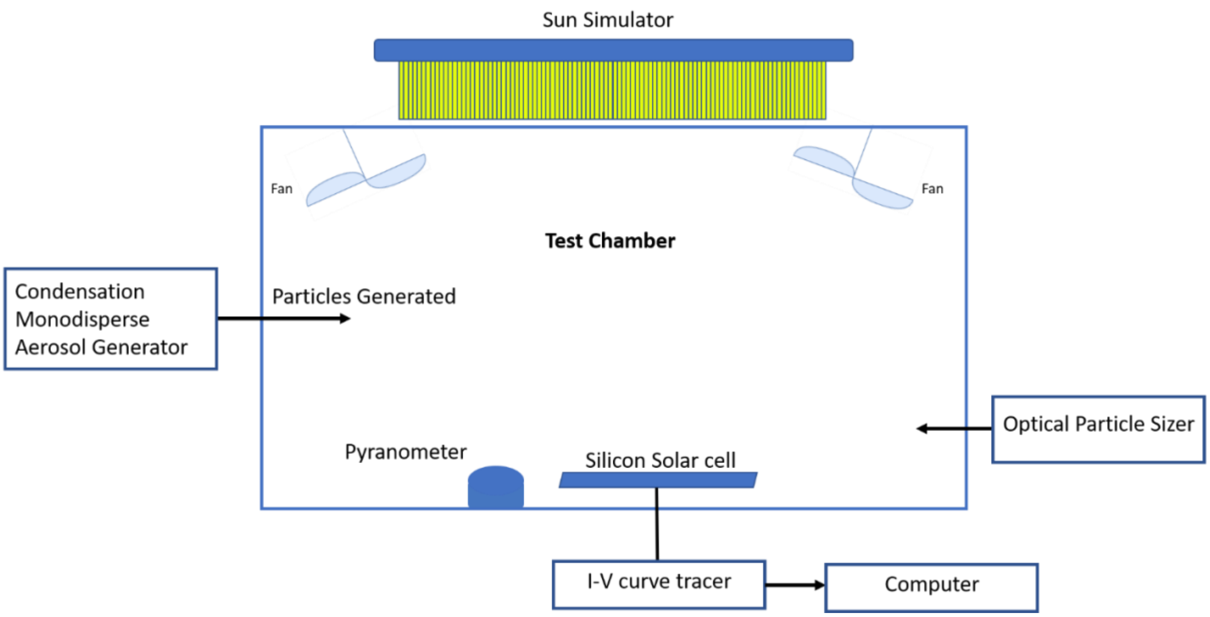

Figure 2. : An illustration of the lab experiment setup (Adapted from (Jiang et al., 2011))

1. Sun Simulator

A solar light simulator (16S-150/300, Solar Light Company, Inc.) was used to provide the input sunlight beaming on the PV module. The maximum output range of the simulated sunlight is 1000 Wm^{-2}. A Class II Pyranometer (PMA2144, PMA2100, Solar Light Company Inc.) was used to measure the irradiance received by the PV cell inside the chamber in order to calculate the input power. The solar irradiance was found to be 735 Wm^{-2} (Figure 3). As Figure 4 shows, the solar cell was placed at an elevation equivalent to that of the sensor of the pyranometer, so that they both receive the same irradiance (735 $W.m^{-2}$).

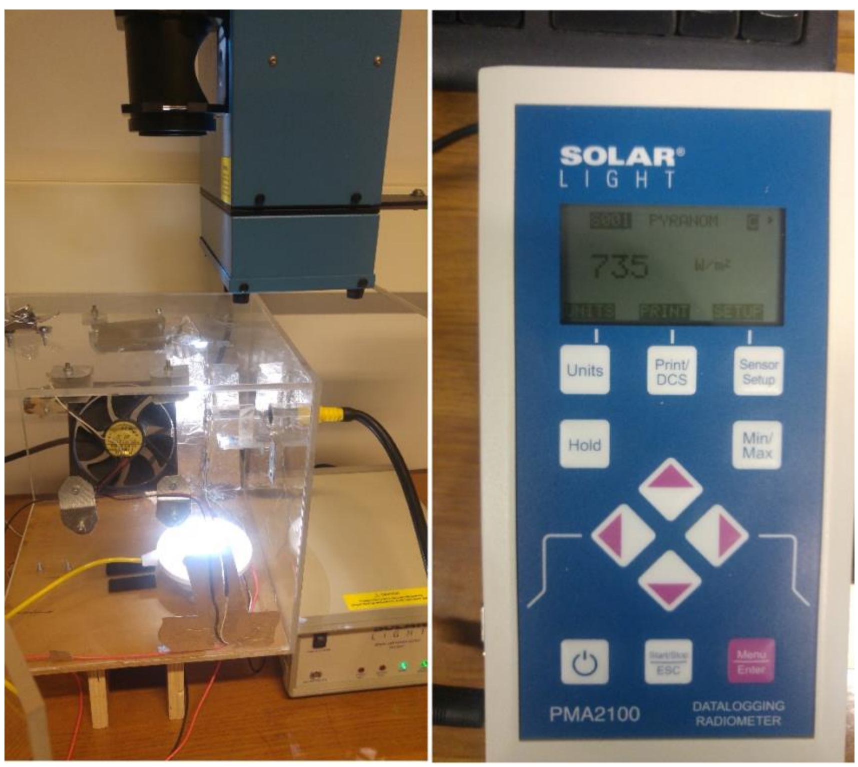

Figure 3: An illustration of how the irradiation was measured inside the chamber by the pyranometer (left) and the corresponding reading of the meter (right)

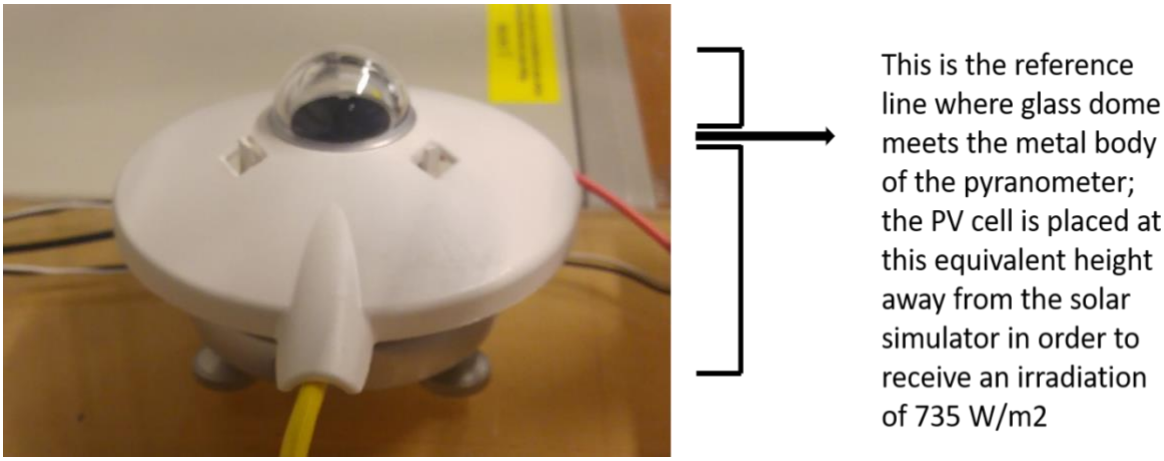

Figure 4: The Class II Pyranometer (PMA2144, PMA2100, Solar Light Company Inc.) used

2. PV System

A static 100 mA 2 cm x 2 cm silicon solar cell (Silicon Reference cell S/N: 18907, Solar Light Company Inc.) was placed inside the chamber and its I-V curve was measured using the Keithley 2400 Source-Meter I-V curve tracer (Model 2400 123456 rev C30) prior to and after dust particle introduction. The power received by the cell, was calculated by multiplying the solar flux (735 W/m^2) by the area of the solar cell. Since the solar cell was kept in the test chamber in an effort not to disturb its location, another 6 cm × 6 cm commercial cell was placed in close proximity and used to measure the mass of the particles deposited on its surface. The mass of the commercial cell was measured twice, once prior to dust generation and once after the experiment was concluded. The mass was assessed using an analytical mass balance (Radwag Model: AS 220.R2 PLUS) with a readability of 0.1 mg, ± 0.2 mg. To get the deposition density, we divide the mass difference (in gram) by the area of the commercial solar cell which is 36 cm^2.

3. Particle Generator or CMAG

A Condensation Monodisperse/Polydisperse Aerosol Generator (CMAG) – TSI 3475 was used to generate particles with different sizes and concentrations in the test chamber. The CMAG is able to generate particles with sizes ranging between 0.1 µm and 10 µm. We used Di-Ethyl-Hexyl-Sebacat (DEHS) as the aerosol material in order to emit particles in the range of 0.1 – 8 µm. DEHS is an insoluble, colorless and odorless liquid, which is used to steadily produce monodispersed aerosols. Particles injected into the test chamber were guaranteed to be properly mixed with the help of two small fans that ran inside the chamber to create a homogenizing effect or a mono-dispersive distribution of dust particles. To operate the CMAG, a nitrogen gas tank was connected, and the tank's valve was opened and adjusted in order to regulate three parameters namely, total flow, saturator flow, and bypass screen flow meters. These three variables control the desired particle size to be generated as summarized in Table 3.

Table 3: Particle generator parameters associated with several size particles

Size	**Temperature**	**Saturator Flow**	**Total flow**	**Screen Bypass flow**	**Aerosol Material**	**NaCl**
2.71 µm	220°C	150 l/h or: Scale = 6	250 l/h or: Scale = 8.75	220 l/h or Scale = 8.1	DEHS	20 mg/l
1.2 µm	180°C	250 l/h or: Scale = 8.75	250 l/h or: Scale = 8.75	0 l/h or Scale = 1	DEHS	20 mg/l
5 µm	240°C	250 l/h or: Scale = 8.75	250 l/h or: Scale = 8.75	0 l/h or Scale = 1	DEHS	20 mg/l
8.5 µm	220°C	250 l/h or: Scale = 8.75	250 l/h or: Scale = 8.75	238.6 l/h or: Scale = 8.6	DEHS	20 mg/l

The particle sizes that were generated from the CMAG ranged from 1.2 to 8 µm. The generation of a particular size was based on the defined CMAG combinations as shown in Table 3. Some of these combinations did not lead to the production of the targeted monodispersed aerosol. Ultimately, the only sizes that were generated were grouped into three general categories, namely S1 for particles with a size less than 1.7 µm, size S2 for particles sized between 1.7 µm and 2 µm, and size S3 with particle sizes ranging between 2 µm and 10 µm. Most of these sizes were generated at three levels of concentrations, namely C1 for low concentration (from 7.88 to 979.5 µg/m^3), C2 for medium concentration (1,026 to 2,899 µg/m^3), and C3 for high concentration (3,422 to 7,302 µg/m^3). Each of the utilized combinations was replicated three times. As such, the total number of runs executed totaled 36. However, the final number of experiments conducted was 46, as several experiments had to be repeated when results showed larger variability.

4. *Optical Particle Sizer Spectrometer or OPS*

The optical particle sizer (OPS) spectrometer (Model 3330 - TSI) was used to monitor the particles' concentrations and size distributions inside the chamber, while particles were being generated. The OPS is able to measure particles from 0.3 to 10 µm in up to 16 user adjustable size channels, with size resolution < 5% at 0.5 µm. It also measures a wide range of concentration from 0 up to 3,000 particles/cm3. As shown in Figure 5, the reading on the OPS at time t = 50 s was recorded for each experimental run. The OPS records two variables namely, the concentration of all particles in the chamber in µg/m3 (e.g. 3,422 µg/m3 in Figure 5) and particles' size with the highest concentration among all particles in the chamber (e.g. 2.5 µg in Figure 5). If the most frequent size was 2 µm, we looked at the second highest size in terms of frequency in order to decide whether the size distribution should be assumed to belong to size S2 or S3; if the position of the second highest bar has a is below 2 µm, then the size distribution was assumed to belong to S2 and if it was higher than 2 µm then the size distribution belonged to S3.

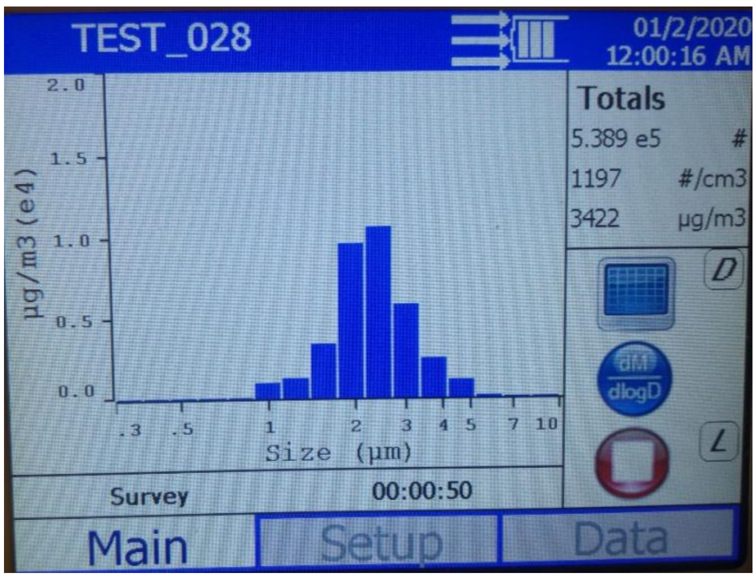

Figure 5: An illustration of the Optical Particle Sizer (OPS) Reading for Test 28

5. Determining the duration of the experiment

Several trials were conducted by varying the durations of particle injection and the allowed time for deposition, all whilst measuring how the efficiency of the solar cells was impacted. It was found that the optimal duration to continuously inject particles was 50 seconds, while the duration for the particles to naturally deposit on the surface of the PV was set to five minutes. This guarantees that the generated aerosols do not evaporate. DEHS droplets with a diameter of 0.3μm have a lifetime of around 4 hours (Topas GmbH, 2019). Following the generation of aerosols for the first 50 seconds, the particle generator and the fans were tuned off and the aerosol concentration and size distribution inside the chamber was captured through the OPS. After the passage of five minutes, a second measurement of the I-V curve was conducted. Once the reading was complete, the experiment was stopped, and the chamber opened to collect the PV cell to assess deposition. The chamber and the solar cells were thoroughly cleaned after each experiment to ensure that no particles remained before a new run was initiated.

6. Efficiency

The power of the cell was calculated using Equation 4, while its energy output efficiency was determined based on Equation 5. Before introducing particles into the chamber, the obtained efficiency of the cell was found to range between 11% and 12.5%.

$$P_{cell} = V_{oc} \times I_{sc} \times FF \qquad \text{Equation 4}$$

Where Voc is the open-circuit voltage, Isc the short-circuit current, and FF the filling factor. Voc is the voltage value when the current changes sign. Isc is the current when the voltage reaches zero, and FF, which is a measure of the squareness of the IV curve was calculated based on Equation 5.

$$FF = \frac{V_{mp} \times I_{mp}}{V_{oc} \times I_{sc}} \qquad \text{Equation 5}$$

Where V_{mp} and I_{mp} stand for the combination of voltage and current where the power is maximum.

$$\mu = \frac{Output\ Power}{Input\ Sunpower} = \frac{V_{oc} \times I_{sc} \times FF}{GA} \qquad \text{Equation 6}$$

Where *G* is the reference irradiation and A is the area of the solar module. In order to get the Power received by the cell, we multiply the solar flux (735 W/m^2) by the area of the solar cell which is 2 cm × 2 cm for the reference silicon solar cell present in the lab (S/N: 18907). This power was calculated as 0.294 Watts. Finally, the efficiency was calculated by dividing the output power by the input power as per Equation 4. Figure 6 shows a typical I-V curve from one of the runs.

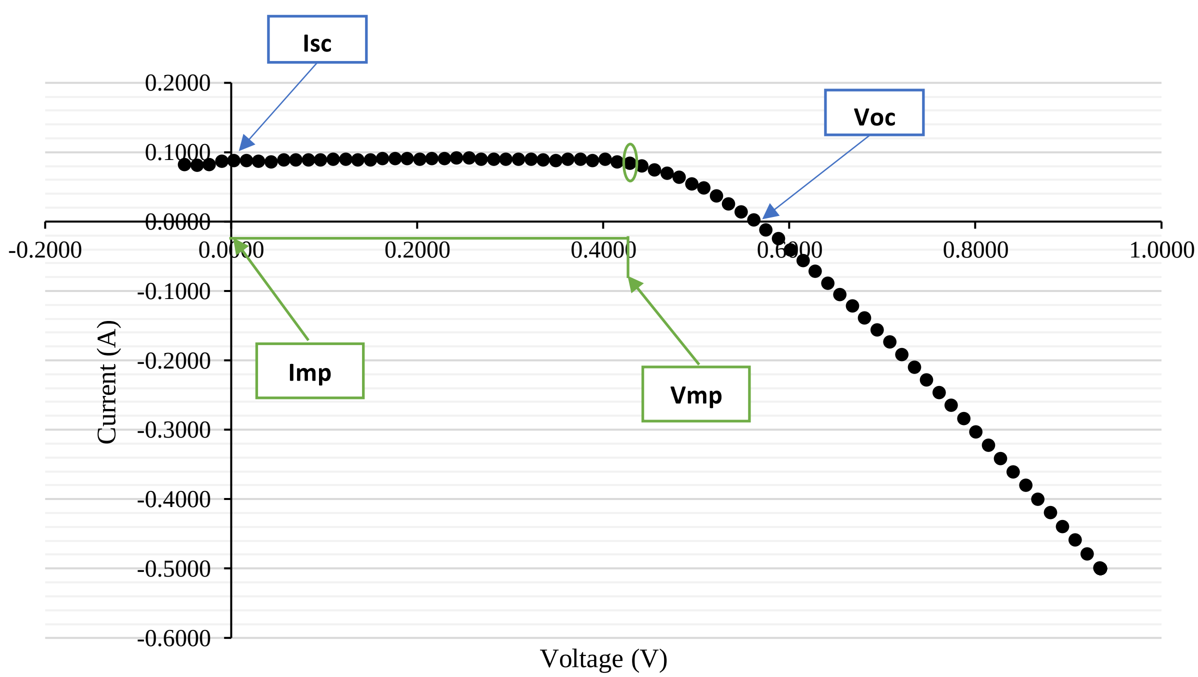

Figure 6: Sample I-V curve for the used silicon cell

For each experimental run, two efficiencies were obtained, one at time t_1 when the solar cell was still clean and another at time t_2 when the solar cell was soiled by the generated dust. The efficiency reduction was calculated as shown below:

$$E_{reduction} = \frac{E_{clean} - E_{dirty}}{E_{clean}}$$ Equation 7

where E_{clean} and E_{dirty} are the output efficiencies before and after dust accumulation respectively.

B. Statistical analysis

Different statistical methods were used including ANOVA tests and regression analysis. ANOVA tests were conducted to assess if the deposition density varied significantly across the three size categories (S1, S2 and S3). Regression models were fitted to quantify the efficiency reduction for each PM size as a function of concentration and deposition density. A logarithmic transformation was applied both to the recorded efficiency and concentration values to reduce their skewness. Size was considered to be a categorical variable. A multiple linear regression model was thus developed to predict the efficiency reduction in the solar panels. The multiple linear regression model can be presented by the equation below.

$$Y = \beta X + e$$ Equation 8

Where **Y** represents a vector of n observations of the response variable 'efficiency reduction'; *X* is a matrix with columns for predictors namely 'the concentration of particles in the air' and 'size of particles'. β is the vector of model coefficients. The multiple linear regression model was developed using a supervised forward selection procedure. The final model was selected based on the highest adjusted-R^2. Predictors that decreased the adjusted-R^2 and/or resulted in other predictors becoming insignificant (with p-value > 0.1) were removed. Predictors with p-values slightly larger than 0.1 were kept in the model if their removal resulted in a large drop in the model performance and if the sign of their coefficient was plausible. Final residual diagnostic tests were applied to check for linearity, influential observations (Cook's D), heteroskedasticity, and non-normality. All the regression models and plots were generated using the R software (R Core Team, 2019).

CHAPTER III

RESULTS AND DISCUSSION

In total, 46 experiments were conducted across the three defined sizes. Of these, 9 experiments were in the size 1 category (<1.7 µm), 27 experiments in the size 2 category (1.7-2 µm), and the remaining 10 were conducted for particles with sizes greater than 2 µm. As mentioned in the methodology, each of the experimental runs was repeated three times. Outliers were identified and censored if one of the measured concentrations, deposition densities, efficiency reductions, or particle sizes was significantly different (more than 2 standard deviations away from the mean) from the values measured for the same combination. In that event, the entire experiment was censored. As a result, 14 experimental runs were excluded from further analysis (3 from size 1; 9 from size 2; and 2 from size 3). The concentration of generated particles in the chamber across all experiments ranged from 7.9 $\mu g/m^3$ to 7,302 $\mu g/m^3$, with 50% of the experiments conducted with concentrations less than 2,018 $\mu g/m^3$. As shown in **Error! Reference source not found.** , the range of the generated concentrations was not the same across the three sizes. The range under S2 and S3 was significantly larger than that of S1, with the widest range across the three size classes observed under S3. This is probably due to the inability of the CMAG to generate small size particles at high concentrations.

In terms of deposition density, the values range from 0.03 g/m^2 to 0.67 g/m^2, with half of the experiments reporting deposition densities less than 0.14 g/m^2. Overall, the deposition density was found to be largely similar across the three sizes (**Error! Reference source not found.**). On the other hand, looking at the effect of concentration on the deposition density

(Figure 7b), there appears to be no clear pattern across the three sizes. This agrees with the findings of Boyle et al. (2016), who found weak correlations between the surface mass accumulation on one hand and $PM_{2.5}$ and PM_{10} concentrations in the air on the other. Nevertheless, several studies have reported that the deposition density tends to be affected by the size of the particles, with larger size particles associated with higher disposition rates (Lu et al., 2016; Micheli et al., 2016; Wang et al., 2020). These studies attributed this relationship to the fact that airborne particles with bigger size are more strongly affected by gravity and as such tend to have a stronger correlation with the soiling ratio.

Moreover, the recoded reduction in the efficiency of the solar cell ranged between 3% and 69%, with an average efficiency reduction of 21% and median of 17%. These reductions agree with the findings of Neher et al. (2017), who reported that aerosols were expected to reduce PV yields between 2% and 48% on average based on their atmospheric radiative transfer and a PV power model. Overall, efficiency reduction increased with particle size and so did the variability in the efficiency reduction (**Error! Reference source not found.**). Overall, we found that efficiency reduction increased as the concentration of particles in the air increased for each of the size classes considered. Yet, the rate of efficiency drop with concentration was size specific (Figure 7). The largest drop in efficiency as a function of concentration was observed for particles in the S3 size category, while the rate of reduction as a function of concentration was lowest for the particles in S1. Yet, this could be due to the small range of concentrations generated under the latter. Additionally, there was no correlation between the recorded deposition rate per particle size and the measured reduction in efficiency (Figure 8).

Table 4: Efficiency reduction and deposition density under the three particle size categories generated

Size	Concentration (µg/m³)			Efficiency Reduction (%)			Deposition density (g/m²)		
	Mean	Min	Max	Mean	Min	Max	Mean	Min	Max
S1(< 1.7 µm)	200	8	529	14.4	8.9	19.3	0.24	0.11	0.36
S2 (1.7 µm - 2 µm)	2,744	175	7,302	16.6	5.8	25.5	0.13	0.03	0.36
S3 (> 2 µm)	2,794	40	5,867	34.7	2.9	69.3	0.28	0.03	0.67

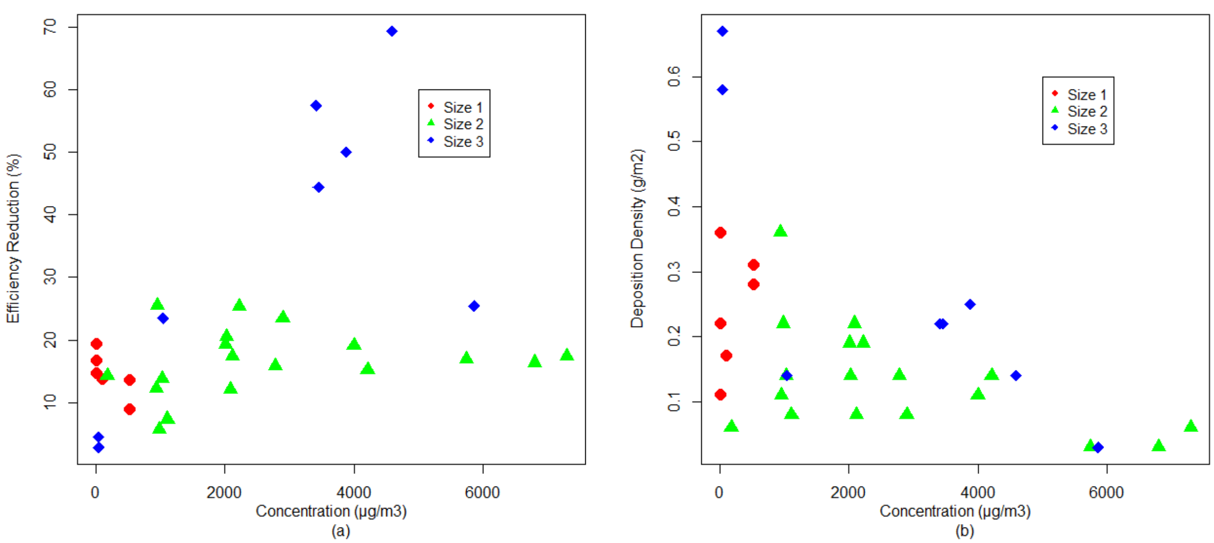

Figure 7: (a) Efficiency reduction as a function of concentration (µg/m³) and particle size; (b) Deposition density (g/m2) as a function of concentration (µg/m³) and particle size

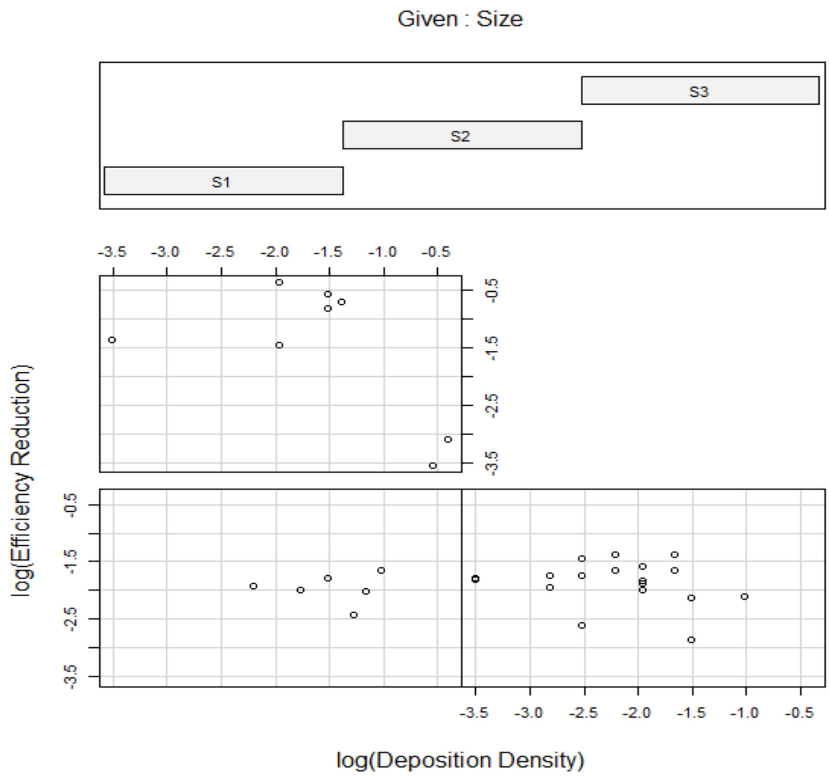

Figure 8: Log of efficiency reduction as a function of log of deposition density

Overall, the reduction in efficiency was found to be a function of concentration and size group. The developed multiple linear regression model showed that the predicted natural logarithm of efficiency reduction varied as a function of the natural logarithm of the concentration of particles and their sizes. The model results indicated that there was a statistically significant interaction between particle size and concentration (**Error! Reference source not found.**). This indicates that the rate at which efficiency dropped as a function of concertation is size dependent. Overall, the model was highly significant (p-value $=2.73\times10^{-7}$) and was able to explain more than 76% of the variability observed in the data. Moreover, the model did not show signs of multicollinearity and overfitting (adjusted

R^2 of the developed model was 0.71). The equation of the regression model is shown in Equation 9. As can be seen from the model, for size S1 the percent drop in efficiency was independent of the measured concentration. For size S2, a 10% increase in concentration results on average in a reduction of efficiency of 2.4%. The equivalent increase in efficiency reduction for particles of size S3 was 6.5%.

$$\begin{cases} \log(\text{Efficiency reduction}) = -1.48 & ;\text{for Size S1} \\ \log(\text{Efficiency reduction}) = -2.88 + 0.13 \times \log(\text{Concentration}) & ;\text{for Size S2} \\ \log(\text{Efficiency reduction}) = -5.29 + 0.54 \times \log(\text{Concentration}) & ;\text{for Size S3} \end{cases} \quad \text{Equation 10}$$

Table 5: Coefficients of the linear regression model

Parameter	Estimate	Std. Error	P-value
Intercept for S1	-1.47	0.38	0.000703 ***
Intercept for S2	-2.88	0.74	0.000591 ***
Intercept for S3	-5.29	0.47	$1.98\text{x}10^{-11}$***
Slope on Log(concentration) for S1	-0.12	0.09	0.182571
Slope on Log(concentration) for S2	0.25	0.13	0.00164***
Slope on Log(concentration) for S3	0.66	0.11	$1.74\text{x}10^{-6}$ ***

Significant codes: 0 '***' 0.001 '**' 0.01 '*' 0.05 '.' 0.1 ' ' 1

Our findings agree with those of Wang et al. (2020), who reported that when the concentration of $PM_{2.5}$ increased by 3.5 times (from 54 µg/m^3 to187 µg/m^3) the power generation capacity dropped by was 34% (dropped from 0.56 kWh to 0.37 kWh). Given that the concentration of the aerosols did not affect the measured deposition density, it is highly likely that increased pollution levels negatively affected light diffusion, which in turn resulted in a drop in efficiency. Several papers have looked closely at the effect of increased air pollution concentrations on light diffusion. Abderrezek and Fathi (2017) showed that the solar spectrum decreased linearly with the increase of dust concentration, thus light became more diffused under glazing. Meanwhile, Alshawaf, Poudineh, and Alhajeri (2020) reported that different PM_{10} concentrations led to different reductions in the total irradiation. They showed that in the event of sandstorms with an average daily PM_{10} concentration below 300 ppb, reductions in the daily total irradiation were negligible. On the other hand, severe sandstorms with PM_{10} concentrations ≥ 2700 ppb led to a 57% reduction in the daily total irradiation. Zhang et al. (2016) found out that for a 1 percent increase in the $PM_{2.5}$ concentration the solar irradiation decreased by 4%, 7% and 9% for the good, slightly polluted and severely polluted groups, respectively. With regards to the effects of particle size on efficincy reduction, several papers have reported that size does matter. For example, J. Kaldellis and Kapsali (2011) studied the effect of different size particles including ash with size less than or equal to 10 µm, limestone with size less than or equal to 60 µm, and red soil with size particles less than or equal to 150 µm through an indoor lab-based experiment. They reported that red soil caused the PV efficiency to be reduced by 2.3%, followed by limestone at 1.2% then carbon ash at 0.7 %. However, El-Shobokshy and Hussein (1993b) studied the effect of limestone-based dust with particle sizes of 80 µm, 60 µm and 50 µm respectively, alongside cement with size of 10 µm and carbon with size of 5 µm. They found that dust with fine particles reduced the performance of PV cells the most.

Several studies have attributed the effect of the dust size on efficiency reduction to the corresponding dust deposition density (Jiang et al., 2011; Wang et al., 2020; Zhang et al., 2016). In our study, the deposition density was also found to depend on the size of the dust particles. The dust deposition for particles in size S2 was found to be siginficalty lower than that at S3 (p-value = 0.013) (Figure 9). The mean deposition density for size S2 particles was 0.13 g/m^2 lower than that of size S3 particles (0.28 g/m^2). Moreover, the deposition density for size S1 was found to be statistically similar to that of S2. This concurs with the results of Lu et al. (2016), who reported that the rate of dust deposition increased from 0.12% to 0.28% as particle size increased from 0.5 μm to 10 μm. Interestingly, they found that the deposition rate then decreased when the dust size increased from 10 μm to 50 μm. Micheli et al. (2016) also found that the soling ratio had a higher correlation with PM_{10} levels (R^2 = 0.95) as compared to $PM_{2.5}$ (R^2 = 0.70).

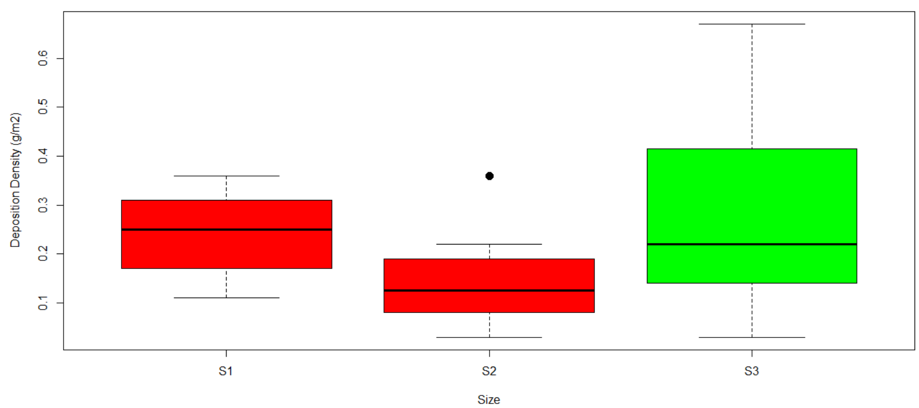

Figure 9: Deposition density for different size particles

CHAPTER IV

CONCLUSION AND LIMITATIONS

Increased concentrations of airborne particulate matter not only affect humans' health but also the performance of photovoltaic power systems (Zhang et al., 2016). PM can significantly influence solar irradiation that can reach solar panels because aerosols scatter incident light and change the state of solar radiation as well as the sky brightness (Sano, Mukai, & Nakata, 2015). In developing countries, PM pollution is more severe in comparison to other countries. In some regions in China, for instance, it has been reported that surface solar radiation has dropped by more than 6% per decade (Liang & Xia, 2005; Qian, Kaiser, Leung, & Xu, 2006). In this study, we investigated the impact of the concentration of particles on the efficiency reduction of solar panels and compared the reductions across three size ranges that were chosen to be within the same size range of $PM_{2.5}$ and PM_{10}. Our results showed that high levels of particle concentration resulted in substantial reductions in the efficiency of solar panels. The reductions ranged between 2.9% and 69.3%. It was also shown that particles with size S3 had the largest effect on the performance of solar panels, with an average efficiency reduction of 34.7% and a maximum efficiency reduction of 69.3%. In comparison, aerosol particles with size S2 were also found to affect the performance of solar panels, leading to an average efficiency reduction of 16.6% and a maximum efficiency reduction of 25.5%. Meanwhile the lowest reductions in efficiency were associated with size S1, resulting in an average efficiency reduction of 14.4% and a maximum efficiency reduction of 19.3%. Moreover, while the study showed clearly that efficiency reduction was a function of concentration and particle size, deposition density proved to be independent of size and concentration. Deposition density across the three sizes ranged between 0.03 g/m^2 and 0.67 g/m^2, with a larger variability in the deposition density observed between sizes S2 and S3. Overall, our results highlight the negative impacts that air pollution has on PV energy production and indicates that future increases in aerosol loads in urban centers are expected to influence PV production on a given site over the lifetime of a PV plant. As such, accounting for the aerosol concentrations at a site is necessary for solar energy assessment (Gutiérrez et al., 2018).

The study faced three main limitations and challenges that need to be addressed in future work. The first was the generation of high particle concentrations in the chamber, which often lead to frequent flow blockages in the optical particle sizer (OPS). Another limitation was the inability of the CMAG to generate high concentrations of particles in size S1. The third was the inability to accurately and directly measure deposition on the PC cell.

REFERENCES

Abderrezek, M., & Fathi, M. (2017). Experimental study of the dust effect on photovoltaic panels' energy yield. *Solar Energy, 142*, 308-320.

Alshawaf, M., Poudineh, R., & Alhajeri, N. S. (2020). Solar PV in Kuwait: The effect of ambient temperature and sandstorms on output variability and uncertainty. *Renewable and sustainable energy reviews*, *134*, 110346.

Bergin, M. H., Ghoroi, C., Dixit, D., Schauer, J. J., & Shindell, D. T. (2017). Large reductions in solar energy production due to dust and particulate air pollution. *Environmental Science & Technology Letters, 4*(8), 339-344.

Boyle, L., Flinchpaugh, H., & Hannigan, M. (2016). Assessment of PM dry deposition on solar energy harvesting systems: measurement–model comparison. *Aerosol Science and Technology*, *50*(4), 380-391.

El-Shobokshy, M. S., & Hussein, F. M. (1993a). Degradation of photovoltaic cell performance due to dust deposition on to its surface. *Renewable Energy, 3*(6-7), 585-590.

El-Shobokshy, M. S., & Hussein, F. M. (1993b). Effect of dust with different physical properties on the performance of photovoltaic cells. *Solar Energy, 51*(6), 505-511.

Fesharaki, V. J., Dehghani, M., Fesharaki, J. J., & Tavasoli, H. (2011). *The effect of temperature on photovoltaic cell efficiency.* Paper presented at the Proceedings of the 1stInternational Conference on Emerging Trends in Energy Conservation–ETEC, Tehran, Iran.

Global Solar Atlas. Retrieved from https://globalsolaratlas.info/

Gutiérrez, C., Somot, S., Nabat, P., Mallet, M., Gaertner, M. Á., & Perpiñán, O. (2018). Impact of aerosols on the spatiotemporal variability of photovoltaic energy production in the Euro-Mediterranean area. *Solar Energy*, *174*, 1142-1152.

IEA Atlas of Energy. Retrieved from http://energyatlas.iea.org/

International Renewable Energy Agency (IRENA). Retrieved from https://irena.org/solar

International Renewable Energy Agency (IRENA). (2018). Renewable Capacity Statistics 2018.

International Renewable Energy Agency (IRENA). (2019). Renewable Capacity Statistics 2019. In.

Jiang, H., Lu, L., & Sun, K. (2011). Experimental investigation of the impact of airborne dust deposition on the performance of solar photovoltaic (PV) modules. *Atmospheric environment, 45*(25), 4299-4304.

Kaldellis, J., & Kapsali, M. (2011). Simulating the dust effect on the energy performance of photovoltaic generators based on experimental measurements. *Energy, 36*(8), 5154-5161.

Kaldellis, J. K., Kapsali, M., & Kavadias, K. A. (2014). Temperature and wind speed impact on the efficiency of PV installations. Experience obtained from outdoor measurements in Greece. *Renewable Energy, 66*, 612-624.

Liang, F., & Xia, X. (2005). Long-term trends in solar radiation and the associated climatic factors over China for 1961-2000.

Lu, H., Lu, L., & Wang, Y. (2016). Numerical investigation of dust pollution on a solar photovoltaic (PV) system mounted on an isolated building. *Applied Energy, 180*, 27-36.

Mani, M., & Pillai, R. (2010). Impact of dust on solar photovoltaic (PV) performance: Research status, challenges and recommendations. *Renewable and sustainable energy reviews, 14*(9), 3124-3131.

Mekhilef, S., Saidur, R., & Kamalisarvestani, M. (2012). Effect of dust, humidity and air velocity on efficiency of photovoltaic cells. *Renewable and sustainable energy reviews, 16*(5), 2920-2925.

Micheli, L., Muller, M., & Kurtz, S. (2016). *Determining the effects of environment and atmospheric parameters on PV field performance.* Paper presented at the 2016 IEEE 43rd Photovoltaic Specialists Conference (PVSC).

Neher, I., Buchmann, T., Crewell, S., Evers-Dietze, B., Pfeilsticker, K., Pospichal, B., . . . Meilinger, S. (2017). Impact of atmospheric aerosols on photovoltaic energy production Scenario for the Sahel zone. *Energy Procedia, 125*, 170-179.

Qian, Y., Kaiser, D. P., Leung, L. R., & Xu, M. (2006). More frequent cloud-free sky and less surface solar radiation in China from 1955 to 2000. *Geophysical Research Letters, 33*(1).

R Core Team. (2019). R: A Language and Environment for Statistical Computing: R Foundation for Statistical Computing. Retrieved from https://www.R-project.org/

Rahman, M., Hasanuzzaman, M., & Rahim, N. (2015). Effects of various parameters on PV-module power and efficiency. *Energy Conversion and Management, 103*, 348-358.

Ramli, M. A., Prasetyono, E., Wicaksana, R. W., Windarko, N. A., Sedraoui, K., & Al-Turki, Y. A. (2016). On the investigation of photovoltaic output power reduction due to dust accumulation and weather conditions. *Renewable Energy, 99,* 836-844.

Roumpakias, E., & Stamatelos, T. (2020). Surface Dust and Aerosol Effects on the Performance of Grid-Connected Photovoltaic Systems. *Sustainability, 12*(2), 569.

Saidan, M., Albaali, A. G., Alasis, E., & Kaldellis, J. K. (2016). Experimental study on the effect of dust deposition on solar photovoltaic panels in desert environment. *Renewable Energy, 92*, 499-505.

Sano, I., Mukai, S., & Nakata, M. (2015). *Retrieval for PM 2.5 distribution from space.* Paper presented at the 2015 IEEE International Geoscience and Remote Sensing Symposium (IGARSS).

Topas GmbH. (2019). Di-Ethyl-Hexyl-Sebacate. Retrieved from https://www.topas-gmbh.de/wordpress/dateien/produkte/DEHS_Datasheet_eng.pdf

Wang, H., Meng, X., & Chen, J. (2020). Effect of air quality and dust deposition on power generation performance of photovoltaic module on building roof. *Building Services Engineering Research and Technology, 41*(1), 73-85.

Zhang, C., Li, W., Yu, J., & Xu, R. (2016). *Modeling impacts of PM 2.5 concentration on PV power outputs.* Paper presented at the 2016 International Conference on Probabilistic Methods Applied to Power Systems (PMAPS).

Zhou, L., Schwede, D. B., Appel, K. W., Mangiante, M. J., Wong, D. C., Napelenok, S. L., . . . Zhang, B. (2019). The impact of air pollutant deposition on solar energy system efficiency: An approach to estimate PV soiling effects with the Community Multiscale Air Quality (CMAQ) model. *Science of The Total Environment, 651*, 456-465.